ground water

Technical Note/

Approximate Solution for Solute Transport during Spherical-Flow Push-Pull Tests

by Martin H. Schroth[1] and Jonathan D. Istok[2]

Abstract

An approximate analytical solution to the advection-dispersion equation was derived to describe solute transport during spherical-flow conditions in single-well push-pull tests. The spherical-flow case may be applicable to aquifer tests conducted in packed intervals or partially penetrating wells. Using results of two-dimensional numerical simulations, we briefly illustrate the applicability of the derived spherical-flow solution and provide a comparison with its cylindrical-flow counterpart. Good agreement between simulated extraction-phase breakthrough curves and the spherical-flow solution was found when the length of the injection/extraction region was small compared to both aquifer thickness and maximum solute frontal position at the end of the injection phase. On the other hand, discrepancies between simulated breakthrough curves and the spherical-flow solution increased with increasing anisotropy in hydraulic conductivities. Several inherent limitations embedded in its derivation such as assumptions of isotropy and homogeneity warrant the cautious use of the spherical-flow solution.

Introduction

Single-well injection-withdrawal tests, which we call "push-pull" tests (PPTs), have been used for the quantitative determination of a wide range of aquifer physical, biological, and chemical characteristics (e.g., Drever and McKee 1980; Gelhar and Collins 1971; Istok et al. 1997). In a PPT, a prepared test solution containing one or more solutes is injected (pushed) into the aquifer using an existing well; the test solution/ground water mixture is then extracted (pulled) from the same location. Aquifer characteristics are determined from an analysis of solute breakthrough curves obtained by measuring solute concentrations at the well during the extraction phase.

Push-pull tracer tests have been used to study physical processes such as advection and dispersion during nonuniform flow. A general form of the advection-dispersion equation for nonuniform flow was developed by Hoopes and Harleman (1967) to study the displacement and mixing of ground water by waste water injected into a single well. Type curves for the analysis of cylindrical-flow fields (one specific form of nonuniform flow) were presented by Sauty (1978), and based on this work, approximate solutions to cylindrical flow were derived by Wang and Crampon (1995). Methods to estimate longitudinal dispersivity from PPTs were developed by Mercado (1966), Gelhar and Collins (1971), and Welty and Gelhar (1994). Based on earlier work by Leap and Kaplan (1988), Hall et al. (1991) derived equations to determine effective porosity and regional ground water velocity from PPTs. The PPTs have also proven useful as a diagnostic tool to quantify matrix diffusion in fractured rock (e.g., Haggerty et al. 2001).

Analytical or semianalytical solutions to solute transport in either diverging or converging flow fields have been derived by several authors (e.g., Chen and Woodside 1988; Novakowski 1992). More recently, a semianalytical solution for solute transport in a sequentially diverging-converging flow field (i.e., during a PPT) was developed by Haggerty et al. (1998). But no fully analytical solution for solute transport during a PPT is available to date as a result of the difficulty of combining the test's diverging flow segment with its converging flow segment. Nevertheless, an approximate analytical solution for

[1]Corresponding author: Institute of Terrestrial Ecology, Swiss Federal Institute of Technology (ETH) Zürich, Grabenstrasse 3, CH-8952 Schlieren, Switzerland; (41) 1-633-6039; fax (41) 1-633-1122; martin.schroth@env.ethz.ch

[2]Department of Civil, Construction, and Environmental Engineering, Oregon State University, 202 Apperson Hall, Corvallis, OR 97331.

Received September 2003, accepted May 2004.

solute transport during a PPT was derived by Gelhar and Collins (1971), which is based on the assumption of cylindrical flow from/to a well screened across the entire saturated thickness of a homogeneous, confined aquifer.

The objective of this note is to present an approximate analytical solution for solute transport during a PPT based on the assumption of spherical flow from/to a well. The spherical-flow case may be applicable to PPTs conducted in packed intervals or partially penetrating wells. Using results from simulated PPTs, we briefly illustrate the applicability of the derived solution and provide a comparison with its cylindrical-flow counterpart.

Theory

General Aspects of Solute Transport during Spherical Flow

The governing equation for one-dimensional solute transport subject to advection, dispersion, and sorption during nonuniform flow in a homogeneous and confined aquifer is (adopted from Bear 1979; Valocchi 1986):

$$\frac{\partial C}{\partial t}+\frac{\rho_b}{n}\frac{\partial S}{\partial t}=\alpha_L|v|\frac{\partial^2 C}{\partial r^2}-v\frac{\partial C}{\partial r} \quad (1)$$

where C and S are solute aqueous-phase and solid (sorbed)–phase concentrations, respectively, ρ_b is bulk density, n is effective porosity, α_L is longitudinal dispersivity, t is time, r is radial distance, and the average pore-water velocity v is a function of r. Equation 1 assumes that molecular diffusion is negligible and mechanical dispersion is a linear function of v (e.g., Bear 1979). Assuming linear equilibrium sorption, a solute retardation factor R can be defined as $R = 1 + \rho_b K_d/n$, where the solute distribution coefficient $K_d = S/C$.

For the case of spherical flow, v is given by:

$$v=\mathrm{d}r/\mathrm{d}t=A/r^2R=Q/4\pi nr^2R \quad (2)$$

with $A = Q/4\pi n$, where Q is the pumping rate (positive during the injection phase and negative during the extraction phase of a PPT). Note that Equation 2 assumes that the regional ground water velocity is negligible compared to the imposed velocity due to pumping.

During the injection phase of a PPT, the solute frontal position $\hat{r}_{inj}$ (Figure 1a) can be obtained by rearranging (separating variables) and integrating Equation 2:

$$\hat{r}_{inj}=\left(\frac{3}{4}\frac{Q_{inj}t_{inj}}{\pi nR}+r_w^3\right)^{1/3} \quad (3)$$

where Q_{inj} is the pumping rate during the injection phase, t_{inj} is time since injection began, and r_w is the injection/extraction well radius. At the end of the injection phase, the solute frontal position attains a maximum value, $\hat{r}_{max}$ (Figure 1b):

$$\hat{r}_{max}=\left(\frac{3}{4}\frac{V_{inj}}{\pi nR}+r_w^3\right)^{1/3} \quad (4)$$

with the total volume injected, $V_{inj} = Q_{inj}T_{inj}$, where T_{inj} is the duration of the injection phase. During the extraction phase, flow is reversed and the frontal position $\hat{r}_{ext}$ is given by (Figure 1b):

$$\hat{r}_{ext}=\left(\hat{r}_{max}^3+\frac{3}{4}\frac{Q_{ext}t_{ext}}{\pi nR}\right)^{1/3} \quad (5)$$

where Q_{ext} is the pumping rate during the extraction phase (not necessarily equal in magnitude to Q_{inj}) and t_{ext} is the time since extraction began. Note that Equation 5 is only meaningful for $|Q_{ext}|t_{ext} \le V_{inj}$. Solute frontal position as specified in Equations 3 through 5 is defined here as the location in the aquifer where $C/C_0 = 0.5$, with C_0 being solute concentration in the injected test solution. Equations 3 through 5 clearly reveal the inverse cubic variation in solute frontal position with time due to the spherical velocity field (Equation 2).

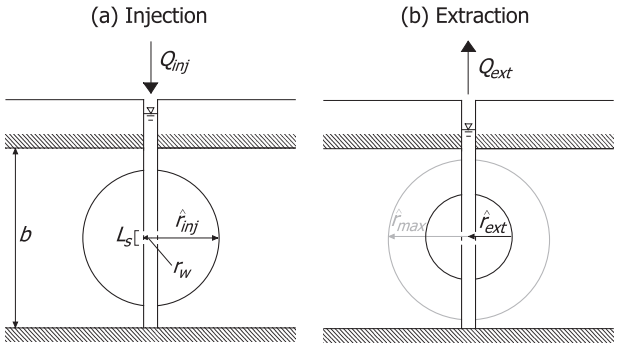

Figure 1. Solute frontal position (C/C_0 = 0.5) during (a) the injection phase and (b) prior to (gray line and label) and during the extraction phase (black line and label) of a PPT conducted under ideal conditions of spherical flow in a homogeneous, confined aquifer. Note that aquifer thickness b is not drawn to scale ($\hat{r}_{max}$ should be substantially smaller than $b/2$).

Approximate Analytical Solution

Gelhar and Collins (1971) derived a general approximate solution for transport of a conservative tracer ($S = 0$, $R = 1$) during nonuniform flow by rewriting Equation 1 in the form of a diffusion equation:

$$\frac{\partial C}{\partial \omega}=\alpha_L\frac{\partial^2 C}{\partial \eta^2} \quad (6)$$

with $\eta = \tau(r) - \hat{t}$

$$\tau(r)=\int_{r_o}^{r} v(r)^{-1}\mathrm{d}r \quad (7)$$

$$\hat{t}=\tau(r) \text{ evaluated at } r=\hat{r} \text{ and} \quad (8)$$

$$\omega=\int_{r_o}^{\hat{r}} v(r)^{-2}\mathrm{d}r \quad (9)$$

where τ is the average travel time for a tracer from the origin r_o to r, $\hat{t}$ is the average travel time for a tracer from r_o to the frontal position $\hat{r}$, and ω accounts for the effects of variable dispersion as a result of the nonuniform velocity field (Welty and Gelhar 1994). For a step change in tracer concentration at the injection/extraction well, i.e., when during a PPT's injection phase, water with $C = 0$ is displaced by the injected test solution with constant

concentration C_0, the general solution to Equation 6 is (Gelhar and Collins 1971):

$$\frac{C}{C_0}=\frac{1}{2}\mathrm{erfc}\left[\frac{\tau-\hat{t}}{(4\alpha_L\omega)^{1/2}}\right] \tag{10}$$

while during the extraction phase of a PPT, the general solution is:

$$\frac{C}{C_0}=\frac{1}{2}\mathrm{erfc}\left[\frac{\hat{t}-\tau}{(4\alpha_L\omega)^{1/2}}\right] \tag{11}$$

Employing the general analysis of Gelhar and Collins (1971), we here derive an approximate analytical solution for solute transport during a PPT based on the assumption of spherical flow from/to a well. Evaluating Equations 7 through 9 for a diverging spherical-flow field yields:

$$\tau=\int_{r_w}^{r}\frac{r^2}{A}\mathrm{d}r=\frac{r^3-r_w^3}{3A} \tag{12}$$

$$\hat{t}=\int_{r_w}^{\hat{r}_{inj}}\frac{r^2}{A}\mathrm{d}r=\frac{\hat{r}_{inj}^3-r_w^3}{3A} \tag{13}$$

$$\omega=\int_{r_w}^{\hat{r}_{inj}}\frac{r^4}{A^2}\mathrm{d}r=\frac{\hat{r}_{inj}^5-r_w^5}{5A^2} \tag{14}$$

where $\hat{r}_{inj}$ is given by Equation 3. By inserting Equations 12 through 14 into Equation 10, we obtain the approximate solution for tracer concentration during the injection phase of a PPT:

$$\frac{C}{C_0}=\frac{1}{2}\mathrm{erfc}\left\{\left(r^3-\hat{r}_{inj}^3\right)\Big/\left[\frac{36}{5}\alpha_L\left(\hat{r}_{inj}^5-r_w^5\right)\right]^{1/2}\right\} \tag{15}$$

Evaluating Equations 7 through 9 for a converging spherical-flow field yields:

$$\tau=\int_{r}^{\hat{r}_{max}}\frac{r^2}{A}\mathrm{d}r=\frac{\hat{r}_{max}^3-r^3}{3A} \tag{16}$$

$$\hat{t}=\int_{\hat{r}_{ext}}^{\hat{r}_{max}}\frac{r^2}{A}\mathrm{d}r=\frac{\hat{r}_{max}^3-\hat{r}_{ext}^3}{3A} \tag{17}$$

$$\omega=\int_{\hat{r}_{ext}}^{\chi}\frac{r^4}{A^2}\mathrm{d}r=-\frac{\hat{r}_{ext}^5}{5A^2}+c \tag{18}$$

where $\hat{r}_{max}$ and $\hat{r}_{ext}$ are given by Equations 4 and 5, respectively, χ is a variable of integration, and c is a constant determined by inserting Equations 16 through 18 into Equation 11 and matching the result with Equation 15 at the end of the injection phase when $\hat{r}_{inj}=\hat{r}_{max}=\hat{r}_{ext}$. This yields the approximate solution for tracer concentration during the PPT's extraction phase:

$$\frac{C}{C_0}=\frac{1}{2}\mathrm{erfc}\left\{\left(r^3-\hat{r}_{ext}^3\right)\Big/\left[\frac{36}{5}\alpha_L\left(2\hat{r}_{max}^5-\hat{r}_{ext}^5-r_w^5\right)\right]^{1/2}\right\} \tag{19}$$

Evaluating Equation 19 at $r=r_w$ and neglecting the well radius, tracer concentration at the well during the extraction phase can be expressed as:

$$\frac{C}{C_0}=\frac{1}{2}\mathrm{erfc}\left\{\left(\frac{V_{ext}}{V_{inj}}-1\right)\Big/\left[\frac{36}{5}\frac{\alpha_L}{\hat{r}_{max}}\left(2-\left|1-\frac{V_{ext}}{V_{inj}}\right|^{2/3}\left(1-\frac{V_{ext}}{V_{inj}}\right)\right)\right]^{1/2}\right\} \tag{20}$$

where the extracted volume $V_{ext}=|Q_{ext}|t_{ext}$. While Equations 15, 19, and 20 were derived for a conservative tracer, they equally apply to solute transport of sorbing solutes during spherical-flow PPTs. Sorbing solutes' retardation behavior is implicitly incorporated in Equations 15, 19, and 20 through $\hat{r}_{inj}$, $\hat{r}_{max}$, and $\hat{r}_{ext}$ (Equations 3 through 5).

To better understand the limitations of Equations 15, 19, and 20, the inherent assumptions embedded in their derivation must be remembered. These include (1) molecular diffusion is negligible; (2) lateral dispersion can be neglected (longitudinal dispersion is much larger than lateral dispersion); (3) steady-state flow is rapidly achieved during injection and extraction phases; and (4) the porous medium is isotropic in hydraulic parameters. Moreover, Equations 15, 19, and 20 are only accurate if $\alpha_L \ll L_o$, where L_o is the total distance traveled by the solute front (Gelhar and Collins 1971).

Example Application

In the following, we present an application of the derived approximate analytical solution for spherical flow. Specifically, we compared Equation 20 and its cylindrical-flow counterpart (equation 42 in Gelhar and Collins 1971)

$$\frac{C}{C_0}=\frac{1}{2}\mathrm{erfc}\left\{\left(\frac{V_{ext}}{V_{inj}}-1\right)\Big/\left[\frac{16}{3}\frac{\alpha_L}{\hat{r}_{max}}\left(2-\left|1-\frac{V_{ext}}{V_{inj}}\right|^{1/2}\left(1-\frac{V_{ext}}{V_{inj}}\right)\right)\right]^{1/2}\right\} \tag{21}$$

with simulated extraction-phase breakthrough curves of hypothetical tracer PPTs conducted in wells screened over only a portion of the saturated thickness of a homogeneous, confined aquifer.

Numerical simulations were conducted using the STOMP code (White and Oostrom 2000), which has been extensively tested and validated against published analytical solutions, as well as other numerical codes (e.g., Nichols et al. 1997). Our computational domain consisted of an array of 1800 nodes distributed in a radial (r)-vertical (z) coordinate system (where z is vertical distance from the base of the aquifer). We used a variable node spacing of $\Delta r = 5$ cm for 2.5 cm $< r <$ 52.5 cm, $\Delta r = 10$ cm for 52.5 cm $< r <$ 202.5 cm, and $\Delta r = 20$ cm for 202.5 cm $< r <$ 302.5 cm, and a uniform node spacing of $\Delta z = 5$ cm for 0 cm $\leq z \leq$ 300 cm. The simulation time-step size varied between 2 and 10 s. Initial conditions were constant hydraulic head for the aqueous phase and $C = 0$ and $S = 0$ for the tracer. Time-varying third-type flux boundary

conditions were used at r_w = 2.5 cm to represent pumping at the injection/extraction well. Zero flux boundary conditions were imposed along the aquifer base (z = 0 cm) and top (z = 300 cm); constant head and zero solute flux boundary conditions at r = 302.5 cm were used to represent aquifer conditions beyond the radius of influence of the well. For all simulations, the total-variation–diminishing scheme was employed (White and Oostrom 2000), which consists of a third-order flux limiter permitting oscillation-free numerical solutions while minimizing numerical dispersion for a wide range of grid Peclet numbers (Gupta et al. 1991).

We performed simulations for a "base case" and nine additional cases, which differed from the base case either in the length of the well screen, L_s, or additionally in the ratio of hydraulic conductivities in r (K_r) and z (K_z) direction, i.e., the ratio $\overline{K} = K_r/K_z$. Base-case parameters (r_w = 2.5 cm, dispersivity in r direction α_r = 2.0 cm, dispersivity in z direction α_z = 0.05 cm, n = 0.4, T_{inj} = 24 h, $Q_{inj} = Q_{ext}$ = 83.3 L/h [V_{inj} = 2000 L], L_s = 10 cm, and $\overline{K}$ = 1) were chosen to represent a typical test conducted in a homogeneous, unconsolidated sand. For case 2, we used L_s = 50 cm, $\overline{K}$ = 1; for cases 3 to 10, we used L_s = 50 cm and varied $\overline{K}$ between 2 and 500.

The duration of the injection phase was selected to give $\hat{r}_{max} \approx 106$ cm for the tracer (Equation 4). Results of the base-case simulation were in excellent agreement with this value, yielding $\hat{r}_{max}$ = 106.5 cm at z = 125 cm (the vertical distance to the center of the well screen, not shown). For this case, we obtained good agreement between the simulated tracer breakthrough curve and the spherical-flow solution (Equation 20, Figure 2a), with a mean-squared error (MSE) of 3.40×10^{-4}. Conversely, agreement between the simulated breakthrough curve and the approximate solution for cylindrical flow (Equation 21) was poor (MSE = 1.03×10^{-2}). This was largely due to the calculation of $\hat{r}_{max}$ in the latter case, which for cylindrical flow is a function of aquifer thickness b: $\hat{r}_{max} = (V_{inj}/\pi bnR + r_w^2)^{0.5}$ (Schroth et al. 2000). Moreover, in the derivation of the cylindrical-flow solution, b is assumed to be equal to L_s (Gelhar and Collins 1971). Thus, base-case parameters would yield $\hat{r}_{max}$ = 399 cm for cylindrical flow, which drastically differed from the actual $\hat{r}_{max}$ = 106.5 cm obtained in our simulation.

Note that all spherical- and cylindrical-flow solutions shown in Figure 2 were computed using simulation input parameters (using $\alpha_L = \alpha_r$), i.e., no fitting of approximate solutions to simulated tracer breakthrough curves was employed. On the other hand, when we optimized α_L for the base-case simulation by fitting the approximate solutions to the simulated tracer breakthrough curve, we obtained for spherical flow α_L = 1.89 cm and for cylindrical flow α_L = 9.61 cm (not shown). Hence, use of the cylindrical-flow solution under circumstances of spherical flow during a PPT led to a severe overestimation of α_r.

For case 2, we obtained reasonable agreement between the simulated tracer breakthrough curve and the spherical-flow solution (Figure 2b). Nonetheless, the MSE value for the spherical-flow solution (7.48×10^{-4}) increased compared to the base-case simulation, while the MSE value for the cylindrical-flow solution (2.35×10^{-3}) decreased. This trend was enhanced in additional simulations, in which L_s was further increased (not shown). Therefore, more accurate results are obtained with the spherical-flow solution when L_s is small compared to $\hat{r}_{max}$ and b.

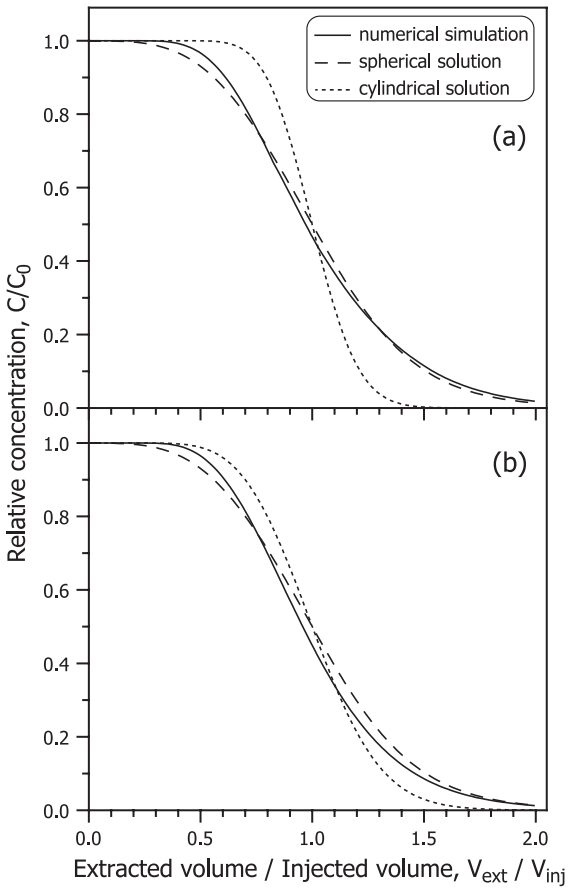

Figure 2. Simulated extraction-phase breakthrough curves for a tracer (solid lines) obtained at the injection/extraction well for (a) base-case (L_s = 10 cm, $\overline{K}$ = 1) and (b) case 2 (L_s = 50 cm, $\overline{K}$ = 1) PPTs in a homogeneous, confined aquifer. Dashed lines show approximate analytical solution for spherical flow (Equation 20), and dotted lines represent approximate analytical solution for cylindrical flow (Equation 21).

In cases 3 to 10, an increase in simulated anisotropy ($2 \leq \overline{K} \leq 500$) led to less agreement between the simulated tracer breakthrough curve and the spherical-flow solution and thus to a monotonic increase in associated MSE values, while MSE values decreased for the cylindrical-flow solution (Figure 3). Less agreement between the simulated tracer breakthrough curve and the spherical-flow solution was mainly caused by changes in $\hat{r}_{max}$, which increased in the simulations from 106.1 cm (for $\overline{K}$ = 1) to a value of 176.9 cm (for $\overline{K}$ = 500) at z = 125 cm (not shown).

Discussion and Conclusions

Despite the demonstrated reasonable agreement between simulated breakthrough curves and the approximate analytical solution for spherical flow under "ideal" conditions (Figure 2a), there are several factors that limit the applicability of the spherical-flow solution. First, for the flow field during a PPT to resemble a spherical-flow pattern (as shown idealized in Figure 1), L_s should be small

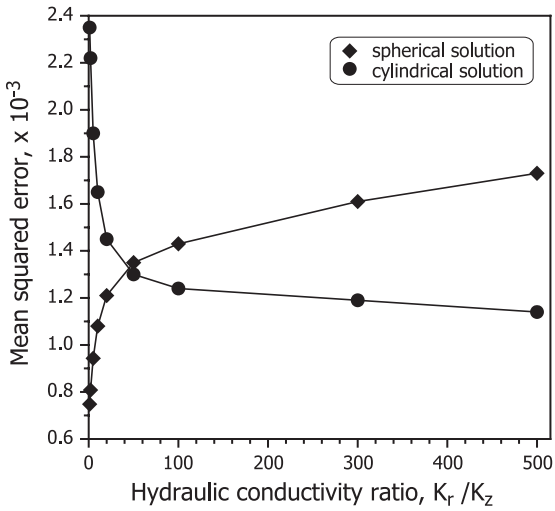

Figure 3. MSEs between simulated tracer breakthrough curves, and approximate analytical solutions for spherical flow [Equation (20)] and cylindrical flow (Equation 21) as a function of porous medium anisotropy in hydraulic conductivities.

compared to $\hat{r}_{\max}$ and b. A relatively large value for $\hat{r}_{\max}$ will also aid in satisfying the requirement of $\alpha_L \ll L_o$. Conversely, $\hat{r}_{\max}$ should be substantially smaller than $b/2$ to prevent solute from reaching aquifer top and bottom boundaries, which would also lead to distortion of the spherical-flow pattern. Second, the derived spherical-flow solution implicitly assumes isotropy in hydraulic parameters, which is rarely encountered in natural settings.

Violation of either factor may cause the flow pattern to approach that of cylindrical flow, i.e., the velocity component in z direction may vanish. Thus, we would clearly expect to obtain less agreement between measured tracer breakthrough curves and the approximate solution for spherical flow for more severe cases of anisotropy (Figure 3). It was beyond the scope of this technical note to assess other inherent assumptions embedded in the derivation of the approximate analytical solution, e.g., the effect of heterogeneities in hydraulic parameters on the accuracy of the spherical-flow solution. Nevertheless, for this case we would expect less agreement with increasing heterogeneity, as was observed for the case of cylindrical flow in PPT simulations performed by Schroth et al. (2000).

Acknowledgments

Special thanks to Mart Oostrom and Mark White, Pacific Northwest National Laboratory, for their continuing support with the STOMP simulator. M.H. Schroth gratefully acknowledges J. Zeyer and the Department of Environmental Sciences, ETH Zürich, for supporting his sabbatical leave at Oregon State University in fall 2001. We also thank C.-S. Chen, an anonymous reviewer, for their comments and suggestions.

Editor's Note: The use of brand names in peer-reviewed papers is for identification purposes only and does not constitute endorsement by the authors, their employers, or the National Ground Water Association.

References

Bear, J. 1979. *Hydraulics of Groundwater.* New York: McGraw-Hill.

Chen, C.-S., and G.D. Woodside. 1988. Analytical solution for aquifer decontamination by pumping. *Water Resources Research* 24, no. 8: 1329–1338.

Drever, J.I., and C.R. McKee. 1980. The push-pull test: A method for evaluating formation adsorption parameters for predicting the environmental effects on in-situ coal gasification and uranium recovery. *In Situ* 4, no. 3: 181–206.

Gelhar, L.W., and M.A. Collins. 1971. General analysis of longitudinal dispersion in nonuniform flow. *Water Resources Research* 7, no. 6: 1511–1521.

Gupta, A.D., L.W. Lake, G.A. Pope, K. Sepehrnoori, and M.J. King. 1991. High-resolution monotonic schemes for reservoir fluid flow simulation. *In Situ* 15, no. 3: 289–317.

Haggerty, R., S.W. Fleming, L.C. Meigs, and S.A. McKenna. 2001. Tracer tests in a fractured dolomite 2. Analysis of mass transfer in single-well injection-withdrawal tests. *Water Resources Research* 37, no. 5: 1129–1142.

Haggerty, R., M.H. Schroth, and J.D. Istok. 1998. Simplified method of "push-pull" test data analysis for determining in situ reaction rate coefficients. *Ground Water* 36, no. 2: 314–324.

Hall, S.H., S.P. Luttrell, and W.E. Cronin. 1991. A method for estimating effective porosity and ground-water velocity. *Ground Water* 29, no. 2: 171–174.

Hoopes, J.A., and D.R.F. Harleman. 1967. Dispersion in radial flow from a recharge well. *Journal of Geophysical Research* 72, no. 14: 3595–3607.

Istok, J.D., M.D. Humphrey, M.H. Schroth, M.R. Hyman, and K.T. O'Reilly. 1997. Single-well, "push-pull" test for in situ determination of microbial activities. *Ground Water* 35, no. 4: 619–631.

Leap, D.I., and P.G. Kaplan. 1988. A single-well tracing method for estimating regional advective velocity in a confined aquifer: Theory and preliminary laboratory verification. *Water Research* 23, no. 7: 993–998.

Mercado, A. 1966. Underground water storage study: Recharge and mixing tests ant Yavne 20 well field. Technical Report 12. Tel Aviv: TAHAL–Water Planning for Israel Ltd.

Nichols, W.E., N.J. Aimo, M. Oostrom, and M.D. White. 1997. STOMP: Subsurface Transport Over Multiple Phases. Application guide PNNL-11216. Richland, Washington D.C.: Pacific Northwest National Laboratory.

Novakowski, K.S. 1992. The analysis of tracer experiments conducted in divergent radial flow fields. *Water Resources Research* 28, no. 12: 3215–3225.

Sauty, J.P. 1978. Identification des paramètres du transport hydrodispersif dans les aquifères par interprétation de traçages en écoulement cylindrique convergent ou divergent. *Journal of Hydrology* 39, no. 1–2: 69–103.

Schroth, M.H., J.D. Istok, and R. Haggerty. 2000. In situ evaluation of solute retardation using single-well push-pull tests. *Advances in Water Resources* 24, no. 1: 105–117.

Valocchi, A.J. 1986. Effect of radial flow on deviations from local equilibrium during sorbing solute transport through homogeneous soils. *Water Resources Research* 22, no. 12: 1693–1701.

Wang, H.Q., and N. Crampon. 1995. Method for interpreting tracer experiments in radial flow using modified analytical solutions. *Journal of Hydrology* 165, no. 1–4: 11–31.

Welty, C., and L.W. Gelhar. 1994. Evaluation of longitudinal dispersivity from nonuniform flow tracer tests. *Journal of Hydrology* 153, no. 1–4: 71–102.

White, M.D., and M. Oostrom. 2000. STOMP. Subsurface Transport Over Multiple Phases, version 2.0, Theory Guide PNNL-12030. Richland, Washington, D.C.: Pacific Northwest National Laboratory.